
Bayesian active learning for closed-loop synaptic characterization

Camille Gontier

Department of Physiology
University of Bern
camille.gontier@unibe.ch

Simone Carlo Surace

Department of Physiology
University of Bern
simone.surace@unibe.ch

Jean-Pascal Pfister

Department of Physiology
University of Bern
jeanpascal.pfister@unibe.ch

Abstract

Model fitting methods have been widely used in neuroscience to infer the parameters of a biophysical system from its responses to experimental stimulations. For instance, the parameters of a chemical synapse can be estimated from its postsynaptic responses to evoked stimuli. However, these estimates critically depend on the stimulation protocol being used. Experiments are often conducted with non-adaptative stimulation protocols that may not yield enough information about the parameters. Here, we propose using Bayesian active learning (BAL) for synaptic characterization, and to choose the most informative stimuli by maximizing the mutual information between the data and the unknown parameters. This requires performing high-dimensional integrations and optimizations in real time. Current methods are either too time consuming, or only applicable to specific models. We build on recent developments in non-linear filtering and parallel computing to provide a general framework for online BAL, which is fast enough to be used in real-time biological experiments and can be applied to a wide range of statistical models. Using synthetic data, we show that our method has the potential to significantly improve the precision of inferred synaptic parameters. Finally, we explore the situation where the constraint is not given by the total number of observations but by the duration of the experiment.

1 Introduction

In most chemical synapses, the postsynaptic responses to presynaptic stimulations are built up of several and similar quanta of current, each of them arising from the release of one presynaptic vesicle [1]. A classical biophysical model used to describe this stochastic release of neurotransmitter is the binomial model: upon the arrival of a presynaptic action potential, vesicles from a pool of N independent release sites open with a probability p , each of these release events giving rise to a quantal current q [2]. In addition, synaptic transmission is also dynamic. Short-term depression (STD) depends on the rate at which vesicles refill during inter-stimulation intervals (ISI). A synapse is thus described by its parameters N, p, q , and by its depression time constant τ_D [3].

These parameters cannot be measured directly, but can be inferred using excitatory postsynaptic currents (EPSCs) recorded on the postsynaptic side and elicited by stimulating the presynaptic cell, a method known as synaptic characterization. For instance, it is possible to use the Expectation-Maximization algorithm to obtain a point-based estimate of the parameters [4], or the Metropolis-Hastings algorithm to compute their full posterior distribution [5]. However, the accuracy of these

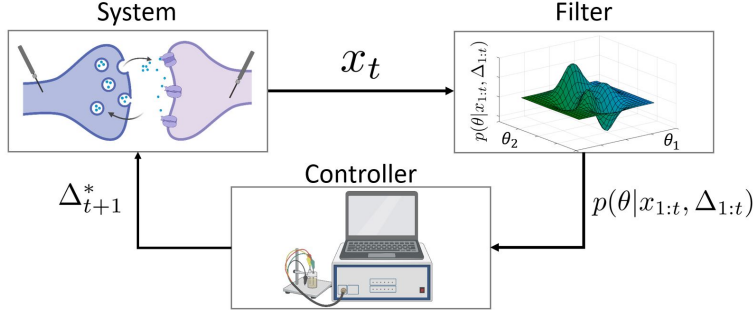


Figure 1: Optimal *infomax* design of experiment using Bayesian active learning. At each time step, the response of the synapse (**system**) to artificial stimulation is recorded. This observation x_t is used by the **filter** to compute the posterior distribution of parameters $p(\theta|x_{1:t}, \Delta_{1:t})$. The **controller** then computes the next stimulation time Δ_{t+1}^* to maximize the expected gain of information. In classical experiment design, the stimulation times $\Delta_{1:T}$ are defined and fixed prior to the recordings.

estimates critically depends on the experimental protocol used for stimulating the presynaptic cell. If observations are noisy or scarce, parameter estimates will be unreliable, leading to identifiability issues [6, 7]. If ISI are longer than the depression time constant τ_D , STD will not be precisely quantified. A Poisson stimulation protocol (in which ISI are drawn from an exponential distribution) provides better estimates of synaptic parameters compared to periodic spike trains with constant ISI, as it spans a broader frequency space [8].

Most experiments still rely on periodic, pre-defined and non-adaptative spike trains, which may not yield enough information about the true parameters. As a consequence, those experiments require more observations, which increases their cost, time, and need for subjects. Here, we propose to apply Bayesian active learning (BAL) to synaptic characterization. Knowing the current estimate of the parameters, the experimental protocol (i.e. the next presynaptic stimulation times) can be optimized on the fly so as to maximize the mutual information between the recordings and the parameters (Figure 1).

Bayesian active learning is a branch of Optimal Experiment Design (OED) theory [9, 10, 11]. It has already been used in neuroscience to infer the parameters of a Generalized Linear Model (GLM) [12], the receptive field of a neuron [13], or the nonlinearity in a linear-nonlinear-Poisson (LNP) encoding model [14]. Implementing BAL for biological settings can be challenging, especially for real-time applications: it requires computing an update of the posterior distribution of parameters after each time step; and using it to compute the expected information gain from future experiments, which involves solving an optimization problem over a possibly high-dimension stimulus space. Different Monte Carlo (MC) methods have been proposed to perform these computations [15, 16], but their computation time can be several orders of magnitude larger than the typical ISI, making them impractical for synaptic characterization.

Our contribution is threefold. Firstly, we provide the first application of Bayesian active learning to synaptic characterization. Stimulation times are computed on the fly in order to maximize the mutual information between the observations and the inferred parameters. Using synthetic data, we show that our method allows to significantly reduce the uncertainty of the estimate in comparison to classically used non-adaptative stimulation protocols. Secondly, we provide a general framework for online active learning, building on recent developments in non-linear filtering [17] and parallel computing [18, 19]. While previous implementations of active learning either relied on time consuming MC methods or were only applicable to special cases, such as linear models or GLM [12], our proposed solution is fast enough to be used in real-time biological experiments and can be applied to many statistical model. Finally, we extend active learning to non-myopic designs. To reduce computational complexity, classical implementations of sequential experiment design usually only optimize for the immediate next observation. This classical myopic approach disregards all future observations in the experiment, and is thus possibly suboptimal [11, 20]. Here, we show that the rate of information gain (in bit/s) of the whole experiment can be optimized by adding a penalty term for longer ISI.

2 Bayesian active learning

When using active learning in sequential experiments, three key elements need to be defined (Figure 1): (1) The **system** to be studied: its parameters θ can be inferred from its observed responses to a set of input stimuli (i.e. the experimental protocol Ψ). Given the stochastic nature of most systems studied in biology, the observations X can take various values x according to a distribution $p(x|\Psi, \theta)$ (see Section 3); (2) A **filter** that computes the posterior distribution of the parameters given the previous inputs and observations $p(\theta|x, \Psi)$: it is updated after each new observation (see Section 4); (3) A **controller** that computes the next input stimuli so as to maximize a certain utility function $U(\Psi)$ (see Section 5). The three following sections will describe each of these elements in detail.

In general, the utility of a given protocol Ψ can be expressed as the mutual information between the parameter random variable Θ and the response random variable X , i.e. $I_\Psi(\Theta; X)$ (see [15, 21] for a detailed discussion). In synaptic characterization, Ψ corresponds to a set of T stimulation times $\Delta_{1:T}$ and observations correspond to recorded EPSCs $x_{1:T}$. In case of successive experiments [13], the mutual information between the parameters and the next observation x_{t+1} conditioned on the previous inputs and observations is:

$$I_{x_{1:t}, \Delta_{1:t}}^{\Delta_{t+1}}(\Theta; X_{t+1}) = H_{x_{1:t}, \Delta_{1:t}}(\Theta) - H_{x_{1:t}, \Delta_{1:t}}^{\Delta_{t+1}}(\Theta|X_{t+1}) \quad (1)$$

where

$$H_{x_{1:t}, \Delta_{1:t}}(\Theta) = - \int d\theta p(\theta|x_{1:t}, \Delta_{1:t}) \log p(\theta|x_{1:t}, \Delta_{1:t})$$

is the entropy of the distribution of Θ at time t ; and

$$H_{x_{1:t}, \Delta_{1:t}}^{\Delta_{t+1}}(\Theta|X_{t+1}) = \int dx_{t+1} p(x_{t+1}|x_{1:t}, \Delta_{1:t+1}) H_{x_{1:t+1}, \Delta_{1:t+1}}(\Theta)$$

is the expected entropy of the distribution of Θ at time $t+1$.

The latter depends on the future observation x_{t+1} which is unknown. We thus take its average over x_{t+1} ; as the predictive distribution depends on the unknown parameters, we also have to take an average over θ , using the current posterior distribution $p(\theta|x_{1:t}, \Delta_{1:t})$ at time t : $p(x_{t+1}|x_{1:t}, \Delta_{1:t+1}) = \int d\theta p(x_{t+1}|x_{1:t}, \Delta_{1:t+1}, \theta) p(\theta|x_{1:t}, \Delta_{1:t})$ [12]. The goal of Bayesian active learning (or infomax design) is to select the next stimulation time to maximize this mutual information (see Figure 1):

$$\Delta_{t+1}^* = \arg \max_{\Delta_{t+1}} I_{x_{1:t}, \Delta_{1:t}}^{\Delta_{t+1}}(\Theta; X_{t+1}) \quad (2)$$

Different methods have been proposed to compute Eq. 1. Monte Carlo (MC) methods [15] or a variational approach [16] can be employed, but they usually require long computation times that can be impractical if the time between successive experiments is short. Closed-form solutions can be computed for some special cases, such as linear models of GLM [12].

3 The system: a binomial model of neurotransmitter release

A classically used model to describe the release of neurotransmitters at chemical synapses is called the binomial model [2, 4, 5, 6, 22, 23]. Under this model, a synapse is described as a Hidden Markov Model (HMM) with the following parameters (units are given in square brackets, see also Figure 2 (a)): N (the number of independent release sites [-]); p (their release probability [-]); σ (the recording noise [A]); q (the quantum of current elicited by one release event [A]); τ_D (the time constant of vesicles refilling [s]). The variables n_t , k_t , and x_t represent, respectively, the number of available vesicles at the moment of spike t , the number of vesicles released after spike t , and the t -th recorded EPSC. For simplicity, we use the notation $p_\theta(\cdot) = p(\cdot|\theta)$ with $\theta = [N, p, q, \sigma, \tau_D]$. The probability

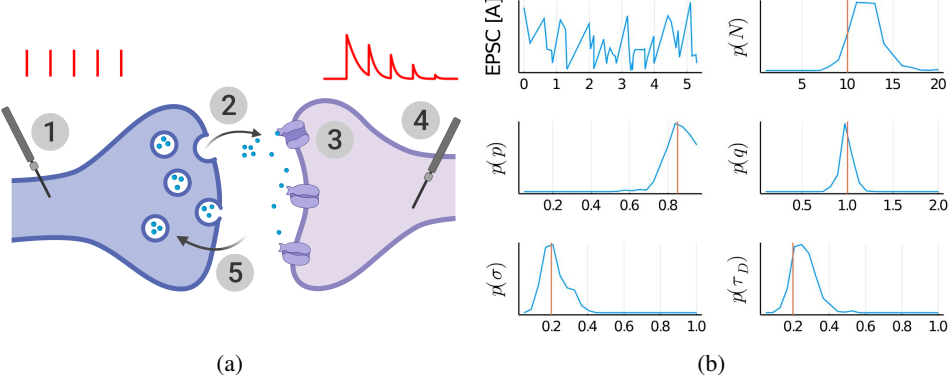


Figure 2: (a) Model of binomial synapse with STD. (1): the presynaptic button is artificially stimulated. (2): After spike t , k_t vesicles (out of the n_t available ones) release their neurotransmitter with a probability p . (3): A single release event triggers a quantal response q . (4): the total recorded postsynaptic response x_t is the sum of the effects of the k_t release events. (5): After releasing, vesicles recover with a time constant τ_D which determines short-term depression. (b) Output of the Nested Particle Filter. Upper left panel: train of synthetic EPSCs generated from model (a). Other panels: posterior distributions of the parameters. Ground-truth values used to generate the EPSCs are displayed as red vertical lines.

of recording $x_{1:T}$ is computed as the marginal of the joint distribution of the observations $x_{1:T}$ and the hidden variables $n_{1:T}$ and $k_{1:T}$:

$$p_\theta(x_{1:T}, n_{1:T}, k_{1:T}) = p_\theta(x_1|k_1)p_\theta(k_1|n_1)p_\theta(n_1) \prod_{t=2}^T p_\theta(x_t|k_t)p_\theta(k_t|n_t)p_\theta(n_t|n_{t-1}, k_{t-1}, \Delta_t) \quad (3)$$

where $p_\theta(x_t|k_t) = \mathcal{N}(x_t; qk_t, \sigma^2)$ is the emission probability, i.e. the probability to record x_t knowing that k_t vesicles released neurotransmitter; $p_\theta(k_t|n_t)$ is the binomial distribution and represents the probability that, given n_t available vesicles, k_t of them will indeed release neurotransmitter: $p_\theta(k_t|n_t) = \binom{n_t}{k_t} p^{k_t} (1-p)^{n_t-k_t}$; and $p_\theta(n_t|n_{t-1}, k_{t-1}, \Delta_t)$ represents the process of vesicles refilling. During the time interval Δ_t , each empty vesicle can refill with a probability $I_t(\Delta_t)$:

$$p_\theta(n_t|n_{t-1}, k_{t-1}, \Delta_t) = \binom{N - n_{t-1} + k_{t-1}}{n_t - n_{t-1} + k_{t-1}} I_t(\Delta_t)^{n_t - n_{t-1} + k_{t-1}} (1 - I_t(\Delta_t))^{N - n_t} \quad (4)$$

with $I_t(\Delta_t) = 1 - \exp\left(-\frac{\Delta_t}{\tau_D}\right)$. Eqs. 3 to 4 define the observation model of the studied system (see Figure 1), i.e. the probability of an observation x_t given a vector of stimuli $\Delta_{1:t}$ and a vector of parameters θ .

4 The filter: online computation of the posterior distributions of parameters

Different methods have been proposed to obtain either a point-based estimate [4] or the full posterior distribution of the synaptic parameters [5] based on observed EPSCs. However, these methods have two main drawbacks. Firstly, their algorithmic complexity scales with N^4 and makes them impractical for studying synapses with a large number of vesicles. Secondly, these methods are not online: the computation time scales with t and thus increases after each new observation [24].

To compute the posterior distribution of parameters $p(\theta|x_{1:t}, \Delta_{1:t})$, we propose to use the Nested Particle Filter (NPF) [17]. This algorithm is asymptotically exact and purely recursive, and thus

allows to directly estimate the parameters as recordings are acquired (see Figure 2 (b)). The NPF relies on two nested layers of particle filtering to approximate the posterior distributions of both the static parameters of the stochastic model and of its hidden states. A first outer filter with M_{out} particles is used to compute the posterior distribution of parameters $p(\theta|x_{1:t}, \Delta_{1:t})$ based on the hidden states n_t and k_t ; and for each of these particles, an inner filter with M_{in} particles is used to estimate the said hidden states (so that the total number of particles in the system is $M_{\text{out}} \times M_{\text{in}}$). After each new observation, these particles are resampled based on their respective likelihoods.

Algorithm 1: NPF [17] for computing one step update of the posterior distribution of parameters

Input: $\{\theta_{t-1}^i\}_{1 \leq i \leq M_{\text{out}}}$, $\{n_{t-1}^{i,j}, k_{t-1}^{i,j}\}_{1 \leq j \leq M_{\text{in}}}$, x_t , Δ_t ;
for i in $1 \dots M_{\text{out}}$ **do**
 Jittering: update the outer particles $\theta_t^i = \kappa(\theta_{t-1}^i)$;
 for j in $1 \dots M_{\text{in}}$ **do**
 Propagation: Draw $n_t^{i,j} \sim p(n_t^{i,j}|n_{t-1}^{i,j}, k_{t-1}^{i,j}, \theta_t^i, \Delta_t)$ and $k_t^{i,j} \sim p(k_t^{i,j}|n_t^{i,j}, \theta_t^i)$;
 Likelihood: compute $\tilde{w}_t^{i,j} = p(x_t|n_t^{i,j}, k_t^{i,j}, \theta_t^i)$;
 end
 Normalization: $\tilde{w}_t^{i,j} \leftarrow \tilde{w}_t^{i,j} / \sum_j \tilde{w}_t^{i,j}$;
 Inner particles resampling: resample $\{n_t^{i,j}, k_t^{i,j}\}_{1 \leq j \leq M_{\text{in}}}$ based on $\{\tilde{w}_t^{i,j}\}_{1 \leq j \leq M_{\text{in}}}$;
end
 Compute $w_t^i = \frac{1}{M_{\text{in}}} \sum_j \tilde{w}_t^{i,j}$;
 Normalization: $w_t^i \leftarrow w_t^i / \sum_i w_t^i$;
 Outer particles resampling: resample $\{\theta_t^i\}_{1 \leq i \leq M_{\text{out}}}$ and $\{n_t^{i,j}, k_t^{i,j}\}_{1 \leq j \leq M_{\text{in}}}$ based on $\{w_t^i\}_{1 \leq i \leq M_{\text{out}}}$;
Output: $\{\theta_t^i\}_{1 \leq i \leq M_{\text{out}}}$, $\{n_t^{i,j}, k_t^{i,j}\}_{1 \leq j \leq M_{\text{in}}}$

Computing the posterior distribution of θ also implies to specify a prior $p(\theta)$ from which the initial particles $\{\theta_0^i\}_{1 \leq i \leq M_{\text{out}}}$ will be drawn. For simplicity, we consider here uniform priors (as in [5, 6]), although the algorithm readily extends to different choices of prior.

The NPF relies on the following approximation to recursively compute the likelihood of each particle. Once the observation x_t has been recorded, the likelihood of particle θ_t^i (with i in $1 \dots M_{\text{out}}$) depends on

$$p(\theta_t^i|x_{1:t}) \propto p(x_t|x_{1:t-1}, \theta_t^i, \Delta_t) p(\theta_t^i|x_{1:t-1}) \quad (5)$$

with

$$p(x_t|x_{1:t-1}, \theta_t^i, \Delta_t) = \sum_{(n,k)_{t-1:t}} p(x_t|n_t, k_t, \theta_t^i) p(n_t, k_t|n_{t-1}, k_{t-1}, \theta_t^i, \Delta_t) p(n_{t-1}, k_{t-1}|x_{1:t-1}, \theta_t^i) \quad (6)$$

If the variance of the jittering kernel κ (which mutates the samples to avoid particles degeneracy and local solutions, see Section 3.2 in [17] for a detailed discussion) is sufficiently small, and hence if $\theta_t^i \approx \theta_{t-1}^i$, the approximation $p(n_{t-1}, k_{t-1}|x_{1:t-1}, \theta_t^i) \approx p(n_{t-1}, k_{t-1}|x_{1:t-1}, \theta_{t-1}^i)$ allows to recursively compute Eq. 5. In practice, the different terms in Eq. 6 are computed as such: $p(x_t|n_t, k_t, \theta_t^i)$ corresponds to the *Likelihood* step of Algorithm 2; $p(n_t, k_t|n_{t-1}, k_{t-1}, \theta_t^i, \Delta_t)$ corresponds to the *Propagation* step; and $p(n_{t-1}, k_{t-1}|x_{1:t-1}, \theta_t^i)$ corresponds to the distribution of hidden states at time $t-1$ (see Section 3.4 in [17] for a detailed explanation).

Contrary to previous methods for fast posterior computation that were only applicable to specific models [12], the NPF can be applied to a broad range of state-space dynamical systems. Moreover, it does not require to approximate the posterior as a Gaussian nor require a time consuming (and possibly unstable) numerical optimization step, while being highly parallelizable and efficient [18, 19]: each posterior update step in Algorithm 1 requires less than 1.8ms on an Nvidia Geforce GTX 1080 Ti GPU.

5 The controller: computation of the optimal next stimulation time

5.1 Mean-field approximation of vesicles dynamics

Our model of the synapse, as defined by Eq. 3 to 4, is a Hidden Markov Model with observations x_t and hidden states n_t and k_t . The predictive distribution $p(x_{t+1}|x_{1:t}, \Delta_{1:t+1}, \theta)$ used in Eq. 1 can be computed using the Baum-Welch algorithm: however, the algorithmic complexity of this forward-backward procedure, which scales with N^4 , makes it impractical for closed-loop applications. Here, we suggest that computation can be massively simplified by using a mean-field approximation of the vesicle dynamics: the analytical mean and variance of hidden and observed variables can be computed using recursive formulae.

Let $r_t \in [0, 1]$ denote the average fraction of release-competent vesicles at the moment of spike t . Its values, given $\theta = [N, p, q, \sigma, \tau_D]$ and $\Delta_{1:t}$, can be iteratively computed (see [4], Eq. (7)) from the equations of the Tsodyks-Markram model [3]: $r_t = 1 - (1 - (1 - p)r_{t-1}) \exp\left(-\frac{\Delta_t}{\tau_D}\right)$ with $r_1 = 1$. It follows that the expected value of the EPSC after spike t is

$$\mathbb{E}(x_t) = r_t N p q \quad (7)$$

Similarly, the variance of the number of available vesicles $\text{Var}(n_t)$ can be computed using the law of total variance: $\text{Var}(n_t) = \mathbb{E}(\text{Var}(n_t|n_{t-1}, k_{t-1})) + \text{Var}(\mathbb{E}(n_t|n_{t-1}, k_{t-1}))$. Since $n_t = n_{t-1} - k_{t-1} + v_t$ with $v_t \sim \text{Bin}(N - n_{t-1} + k_{t-1}, I_t)$, it follows that $\text{Var}(n_t) = I_t(1 - I_t)N(1 - r_{t-1} + p r_{t-1}) + (1 - I_t)^2 \text{Var}(n_{t-1} - k_{t-1})$.

Finally, by noting that $(n_t - k_t)|n_t \sim \text{Bin}(n_t, 1 - p)$ and using again the law of total variance to compute $\text{Var}(n_{t-1} - k_{t-1}) = \mathbb{E}(\text{Var}(n_{t-1} - k_{t-1}|n_{t-1})) + \text{Var}(\mathbb{E}(n_{t-1} - k_{t-1}|n_{t-1}))$, we obtain

$$\text{Var}(x_t) = \sigma^2 + q^2(N r_t p (1 - p) + \text{Var}(n_t) p^2) \quad (8)$$

5.2 Computation of the optimal next stimulation time

The objective of experiment design optimization is to minimize the uncertainty of the estimates (which can be quantified using the variance or the entropy) while reducing the cost of experimentation (defined as the number of required trials, samples, or observations). From the experimentalist point of view, a burning question is how to optimize the stimulation protocol such that the measured EPSCs are most informative about the synaptic parameters. Previous studies showed that some stimulation protocols are more informative than others, but ignored the temporal correlations of the number of ready releasable vesicles [8] or did not compute which protocol would be the most informative [4].

The optimal next stimulation time Δ_{t+1}^* that will maximize the mutual information (i.e. minimize the uncertainty about θ as measured by the entropy) can be written from Eq. 1 and 2 as

$$\Delta_{t+1}^* = \arg \min_{\Delta_{t+1}} \int d\theta p(\theta|x_{1:t}, \Delta_{1:t}) \int dx_{t+1} p(x_{t+1}|\Delta_{1:t+1}, \theta) H_{x_{1:t}, \Delta_{1:t}}^{\Delta_{t+1}}(\Theta|X_{t+1} = x_{t+1}) \quad (9)$$

Eq. 9 requires to compute two (possibly high-dimensional) integrals over θ and x_{t+1} , for which closed-form expressions only exist for specific models. To avoid long MC simulations, we propose the following point-based approximations. Firstly, instead of computing the full expectation over $p(\theta|x_{1:t}, \Delta_{1:t})$, we set θ to its maximum a posteriori (MAP) value $\hat{\theta} = \arg \max_{\theta} p(\theta|x_{1:t}, \Delta_{1:t})$. Eq. 9 thus becomes

$$\Delta_{t+1}^* \approx \arg \min_{\Delta_{t+1}} \int dx_{t+1} p(x_{t+1}|\Delta_{1:t+1}, \hat{\theta}) H_{x_{1:t}, \Delta_{1:t}}^{\Delta_{t+1}}(\Theta|X_{t+1} = x_{t+1})$$

Secondly, instead of computing the full expectation over the future observation, we set x_{t+1} to its mean posterior given $\hat{\theta}$ and $\Delta_{1:t+1}$ using Eq. 7, giving:

$$\Delta_{t+1}^* \approx \arg \min_{\Delta_{t+1}} H_{x_{1:t}, \Delta_{1:t}}^{\Delta_{t+1}}(\Theta|X_{t+1} = \mathbb{E}(x_{t+1}))$$

Algorithm 2: Computation of the optimal next stimulation time

```
set  $\hat{\theta} = \arg \max_{\theta} p(\theta|x_{1:t}, \Delta_{1:t})$  (MAP values from the current posterior estimation);  
define  $\mathcal{S}$  (set of candidates  $\Delta_{t+1}$ );  
for  $\Delta_{t+1}$  in  $\mathcal{S}$  do  
    | Compute  $\mathbb{E}(x_{t+1})$  using Eq. 7;  
    | Compute  $H_{x_{1:t}, \Delta_{1:t}}^{\Delta_{t+1}}(\Theta|X_{t+1} = \mathbb{E}(x_{t+1}))$  using Algorithm 1;  
end  
 $\Delta_{t+1}^* = \arg \min_{\Delta_{t+1} \in \mathcal{S}} H_{x_{1:t}, \Delta_{1:t}}^{\Delta_{t+1}}(\Theta|X_{t+1} = \mathbb{E}(x_{t+1}))$ 
```

For each candidate Δ_{t+1} in a given finite set \mathcal{S} , the expected posterior entropy $H_{x_{1:t}, \Delta_{1:t}}^{\Delta_{t+1}}(\Theta|X_{t+1} = \mathbb{E}(x_{t+1}))$ can be computed using Algorithm 1. As results for different candidates Δ_{t+1} are independent, this step can be further parallelized over the elements in \mathcal{S} , and its computation time will only scale with that of Algorithm 1.

6 Results

6.1 First setting: reducing the uncertainty of estimates for a given number of observations

Although crude, the point-based approximations used in Algorithm 2 allow, for a given number of observations, to significantly reduce the uncertainty (as measured by the entropy) of the parameter estimates compared to other stimulation protocols, while being sufficiently fast for online applications. For simplicity, we focus on optimizing the inference of τ_D , since it is usually harder than other parameters to infer precisely and critically depends on the ISI [4, 8]. We compare our implementation of active learning to the following protocols: in the *Constant* protocol, the synapse is probed at a constant frequency $\Delta_t = \text{cst}$; in the *Uniform* protocol, ISI are uniformly drawn from a set \mathcal{S} of candidates Δ_t consisting of equidistantly separated values ranging from $\Delta_t^{\min} = 0.005s$ (i.e. one order of magnitude shorter than the shortest ISI used in [4]) to Δ_t^{\max} ; finally, in the *Poisson* protocol, ISI are drawn from an exponential distribution with mean τ . Such a protocol had been shown to provide better estimates of synaptic parameters compared to periodic spike trains with constant ISI [4, 8].

The efficiency of these protocols will depend on their respective parametrizations. Figure 3 (a) shows the average final entropy decrease (i.e. the information gain) after 200 observations using the *Constant* (top), *Uniform* (middle), or *Poisson* (bottom) protocol, for different values of their parameters. Vertical red lines indicate the ground truth value $\tau_D^* = 0.2s$ used for simulations. If ISI are longer than the depression time constant τ_D^* , STD will not be precisely quantified, and the inferred parameter will be unreliable. The optimal ISI to be used in the *Constant* protocol is thus of the same order of magnitude as τ_D^* . Conversely, the optimal parameters for the *Uniform* and *Poisson* protocols should be larger than τ_D^* , so as to span a broader frequency space.

These classical protocols (with their optimal respective parametrizations) are compared to Bayesian active learning implementing Algorithm 2. \mathcal{S} ranges from 0.005s to 2s (i.e. one order of magnitude higher than τ_D^*). Results are displayed in Figure 3 (b). For the different protocols, the average (over 400 independent repetitions) entropy of the posterior distribution of τ_D is plotted as a function of the number of observations. The NPF requires a minimum number of observations to converge (see Figure 2 (b)). Once it has converged to a reliable estimate of the parameters and hence $\hat{\theta} \approx \theta^*$ (i.e. after ~ 100 observations), active learning outperforms other protocols.

It should be noted that in Figure 3 (b) online active learning is compared to other protocols whose respective parameters have been optimized offline. In real physiology experiments, classical protocols are non-adaptive and are defined using (possibly sub-optimal) default parameters. In contrast, in active learning the protocol is optimized on the fly as data are recorded, and its performance will not depend on a prior parametrization. Finally, our online implementation of active learning (purple line in Figure 3 (b)) is compared to exact active learning (black dashed line), in which Eq. 9 is computed exactly using MC samples. Samples to compute the expectation over θ are drawn from $p(\theta|x_{1:t}, \Delta_{1:t})$, while samples used to compute the expectation over x_{t+1} are drawn from a normal distribution with mean $\mathbb{E}(x_{t+1})$ (Eq. 7) and variance $\text{Var}(x_{t+1})$ (Eq. 8). This shows that

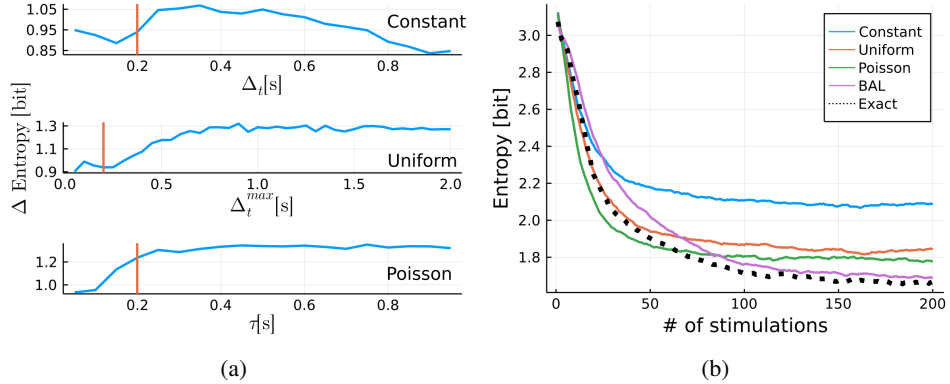


Figure 3: Simulated experiment. **(a)** Average information gain after 200 observations for different parametrizations of the *Constant* (top), *Uniform* (middle), and *Poisson* (bottom) protocols. Red vertical lines show the ground truth $\tau_D^* = 0.2$ s. **(b)** Entropy of the posterior distribution of τ_D vs. number of observations for different stimulation protocols: *Constant* (blue), *Uniform* (red), *Poisson* (green), and online Bayesian active learning (purple). Dashed black line: exact active learning from Eq. 9. Synthetic data were generated from a model of synapse with ground truth parameters $N^* = 10$, $p^* = 0.85$, $q^* = 1$ A, $\sigma^* = 0.2$ A, and $\tau_D^* = 0.2$ s. Traces show average over 400 independent repetitions.

the approximations used in Algorithm 2 to make active learning online only have a small effect on performance.

6.2 Second setting: reducing the uncertainty of estimates for a given experiment time

Active learning allows, for a given number of observations, to improve the reliability of the estimated parameters. However, in its classical implementation, only the next stimulus input is optimized, disregarding all future observations in the experiment. This myopic approach is thus suboptimal. Moreover, neurophysiology experiments are not only constrained by the number of observations, but also by the total time of the experiment. Since cells have a limited life time after they start being probed, the total time of an experiment protocol $\sum_{t=1}^T \Delta_t$ also needs to be accounted for.

Optimizing all stimulation times (for a given experiment end time) would be an intractable problem (especially for online applications), since the algorithmic complexity would scale exponentially with the number of observations. Here, to account for the total time of the experiment, and to globally optimize the information gain per unit of time, we propose to modify the classical formulation of active learning (Eq. 9) by adding a penalty term for longer ISI:

$$\Delta_{t+1}^{*(\eta)} = \arg \min_{\Delta_{t+1}} \left\{ \eta \Delta_{t+1} + \int d\theta p(\theta|x_{1:t}, \Delta_{1:t}) \int dx_{t+1} p(x_{t+1}|\Delta_{1:t+1}, \theta) H_{x_{1:t}, \Delta_{1:t}}^{\Delta_{t+1}}(\Theta|x_{t+1}) \right\} \quad (10)$$

The effect of the penalty weight η on the entropy of the posterior distribution of τ_D is displayed in Figure 4 (a). As expected, adding a penalty term to Eq. 9 reduces the precision of the inferred parameter. The loss of information gain increases with the penalty weight η . However, increasing η also increases the speed of information gain, as seen on Figure 4 (b). Depending on the available time for the experiment, it is thus possible to tune η so as to find a trade-off between precision (Figure 4 (a)) and information rate (Figure 4 (b)).

7 Discussion

The use of non-adaptative protocols in physiology experiments often leads to a large variance of the estimated parameters, even when using a large number of trials or data points. Applying Bayesian

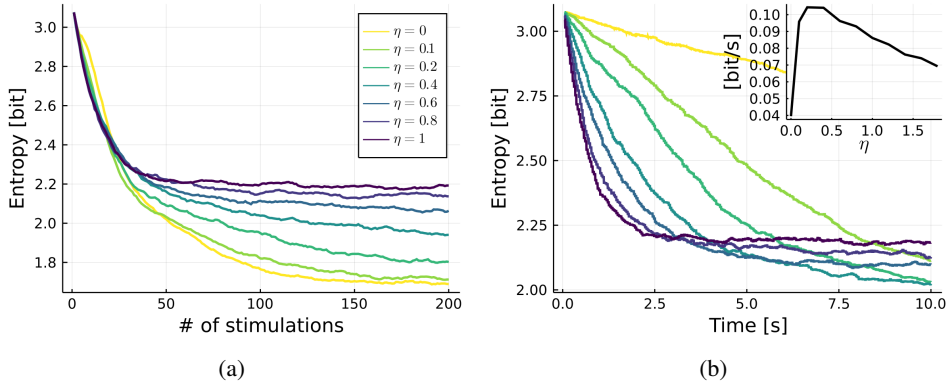


Figure 4: Effect of penalizing long ISI on parameter estimates uncertainty and rate of information gain. (a) Entropy of the posterior distribution of τ_D vs. number of observations for different values of η in Eq. 10. Same settings as in Figure 3. (b) Same results, but displayed as a function of time. Inset: slope of the entropy vs. time curves (i.e. information rate) vs. η after 10 seconds.

active learning allows to reduce the uncertainty of inferred parameters when studying a statistical model. Our main contribution is to use the NPF for the filter, and to apply mean-field approximations for the controller: the result is a proposed framework for active learning which is general and sufficiently fast to be applied to a wide range of physiology experiments. For instance, it can be used to infer the parameters of a GLM, a LNP, or behavioral models. Here, we use it to infer the parameters of a model of synapse. For this specific example, the computation time is a critical constraint, since the typical ISI is usually shorter than 1s.

We expect active learning to be particularly beneficial to neurophysiology experiments involving live cells or subjects. By reducing the number of samples required to obtain a certain result or improving the efficiency of information gain, we can reduce the cost of the experiment and the need for animal subjects. A possible negative impact would be that improving the relative efficiency of neurophysiology experiments may lead to a larger field of applications and therefore a larger demand for animal experiments, analogously to Jevons Paradox [25].

Applying our online active learning algorithm to real recordings is currently still a work in progress. This requires to set up a real-time hardware and software pipeline, and to modify classical experimental apparatus so as to modify scheduled spike trains on the fly. However, previous studies have already illustrated that applying active learning to real neural data is realistic [12, 13, 14]. Moreover, as the Nested Particle Filter is robust to time-varying parameters and model uncertainties [17], we believe that our proposed solution will be particularly relevant for neurophysiology experiments.

Our approach has some limitations. An evident drawback of a weighted method such as the Nested Particle Filter is that it requires a very large number of particles to provide low variance estimates, as the approximation error only decreases with the square root of the number of particles. Moreover, we apply our solution to a simplified model of chemical synapse, which includes neither short-term facilitation [4, 5, 6, 8] nor vesicle content variability [26, 27]. Given the complexity of presynaptic vesicles dynamics, characterizing STD with a single time constant might be an oversimplification [28]. Finally, we lack theoretical results on the convergence of the estimators when using active learning. When observations are independent and identically distributed (i.i.d.), active learning will give an unbiased estimate of the parameters, which variance will decrease with the number of observations [29]. Here, EPSCs are correlated, which may induce information saturation [30] or biased estimates.

Overall, we expect our proposed solution to pave the way towards better estimates of stochastic models in neuroscience. Especially, applying it to synaptic characterization would allow to better understand the role of synaptic transmission in learning and memory [31], to study the role of synaptic stochasticity [32, 33], and lead to an improved understanding of synaptic homeostasis [34, 35], plasticity [36, 37, 38], and connectivity [39].

Acknowledgments and Disclosure of Funding

The work presented in this paper was supported by the Swiss National Science Foundation under grant number 31003A_175644 entitled "Bayesian Synapse".

Figures were created using BioRender. Calculations were performed on UBELIX (<http://www.id.unibe.ch/hpc>), the HPC cluster at the University of Bern. The CUDA.jl package [18, 19] is licensed under the MIT "Expat" License (<https://github.com/JuliaGPU/CUDA.jl/blob/master/LICENSE.md>). We thank Ehsan Abedi, Jakob Jordan, and Anna Kutschireiter for the fruitful discussions.

JULIA files are available in the following package: <https://github.com/Theoretical-Neuroscience-Group/BinomialSynapses.jl>

References

- [1] J Del Castillo and B3 Katz. Quantal components of the end-plate potential. *The Journal of physiology*, 124(3):560–573, 1954.
- [2] Bernard Katz. The release of neural transmitter substances. *Liverpool University Press*, pages 5–39, 1969.
- [3] Misha Tsodyks, Klaus Pawelzik, and Henry Markram. Neural networks with dynamic synapses. *Neural computation*, 10(4):821–835, 1998.
- [4] Alessandro Barri, Yun Wang, David Hansel, and Gianluigi Mongillo. Quantifying repetitive transmission at chemical synapses: a generative-model approach. *Eneuro*, 3(2), 2016.
- [5] Alex D Bird, Mark J Wall, and Magnus JE Richardson. Bayesian inference of synaptic quantal parameters from correlated vesicle release. *Frontiers in computational neuroscience*, 10:116, 2016.
- [6] Camille Gontier and Jean-Pascal Pfister. Identifiability of a binomial synapse. *Frontiers in computational neuroscience*, 14:86, 2020.
- [7] Franz-Georg Wieland, Adrian L Hauber, Marcus Rosenblatt, Christian Tönsing, and Jens Timmer. On structural and practical identifiability. *Current Opinion in Systems Biology*, 2021.
- [8] Rui P Costa, P Jesper Sjostrom, and Mark CW Van Rossum. Probabilistic inference of short-term synaptic plasticity in neocortical microcircuits. *Frontiers in computational neuroscience*, 7:75, 2013.
- [9] Ashley F Emery and Aleksey V Nenarokomov. Optimal experiment design. *Measurement Science and Technology*, 9(6):864, 1998.
- [10] Paola Sebastiani and Henry P Wynn. Maximum entropy sampling and optimal bayesian experimental design. *Journal of the Royal Statistical Society: Series B (Statistical Methodology)*, 62(1):145–157, 2000.
- [11] Elizabeth G Ryan, Christopher C Drovandi, James M McGree, and Anthony N Pettitt. A review of modern computational algorithms for bayesian optimal design. *International Statistical Review*, 84(1):128–154, 2016.
- [12] Jeremy Lewi, Robert Butera, and Liam Paninski. Sequential optimal design of neurophysiology experiments. *Neural computation*, 21(3):619–687, 2009.
- [13] Mijung Park and Jonathan Pillow. Bayesian active learning with localized priors for fast receptive field characterization. *Advances in neural information processing systems*, 25:2348–2356, 2012.
- [14] Mijung Park, Greg Horwitz, and Jonathan W Pillow. Active learning of neural response functions with gaussian processes. In *NIPS*, pages 2043–2051. Citeseer, 2011.
- [15] Xun Huan and Youssef M Marzouk. Simulation-based optimal bayesian experimental design for nonlinear systems. *Journal of Computational Physics*, 232(1):288–317, 2013.
- [16] Adam Foster, Martin Jankowiak, Eli Bingham, Paul Horsfall, Yee Whye Teh, Tom Rainforth, and Noah Goodman. Variational bayesian optimal experimental design. *arXiv preprint arXiv:1903.05480*, 2019.
- [17] Dan Crisan, Joaquin Miguez, et al. Nested particle filters for online parameter estimation in discrete-time state-space markov models. *Bernoulli*, 24(4A):3039–3086, 2018.

- [18] Tim Besard, Christophe Foket, and Bjorn De Sutter. Effective extensible programming: Unleashing Julia on GPUs. *IEEE Transactions on Parallel and Distributed Systems*, 2018.
- [19] Tim Besard, Valentin Churavy, Alan Edelman, and Bjorn De Sutter. Rapid software prototyping for heterogeneous and distributed platforms. *Advances in Engineering Software*, 132:29–46, 2019.
- [20] Christopher C Drovandi, Minh-Ngoc Tran, et al. Improving the efficiency of fully bayesian optimal design of experiments using randomised quasi-monte carlo. *Bayesian Analysis*, 13(1):139–162, 2018.
- [21] Dennis V Lindley. On a measure of the information provided by an experiment. *The Annals of Mathematical Statistics*, pages 986–1005, 1956.
- [22] Christian Stricker and Stephen J Redman. Quantal analysis based on density estimation. *Journal of neuroscience methods*, 130(2):159–171, 2003.
- [23] Volker Scheuss and Erwin Neher. Estimating synaptic parameters from mean, variance, and covariance in trains of synaptic responses. *Biophysical journal*, 81(4):1970–1989, 2001.
- [24] Ola Bykowska, Camille Gontier, Anne-Lene Sax, David W Jia, Milton Llera Montero, Alex D Bird, Conor Houghton, Jean-Pascal Pfister, and Rui Ponte Costa. Model-based inference of synaptic transmission. *Frontiers in synaptic neuroscience*, 11:21, 2019.
- [25] William Stanley Jevons. The coal question. *An Inquiry Concerning the Prog*, 1862.
- [26] Gardave Singh Bhumbra and Marco Beato. Reliable evaluation of the quantal determinants of synaptic efficacy using bayesian analysis. *Journal of neurophysiology*, 109(2):603–620, 2013.
- [27] Cary Soares, Daniel Trotter, André Longtin, Jean-Claude Béïque, and Richard Naud. Parsing out the variability of transmission at central synapses using optical quantal analysis. *Frontiers in synaptic neuroscience*, 11:22, 2019.
- [28] Grant F Kusick, Morven Chin, Sumana Raychaudhuri, Kristina Lippmann, Kadidia P Adula, Edward J Hujber, Thien Vu, M Wayne Davis, Erik M Jorgensen, and Shigeki Watanabe. Synaptic vesicles transiently dock to refill release sites. *Nature neuroscience*, 23(11):1329–1338, 2020.
- [29] Liam Paninski. Asymptotic theory of information-theoretic experimental design. *Neural Computation*, 17(7):1480–1507, 2005.
- [30] Rubén Moreno-Bote, Jeffrey Beck, Ingmar Kanitscheider, Xaq Pitkow, Peter Latham, and Alexandre Pouget. Information-limiting correlations. *Nature neuroscience*, 17(10):1410–1417, 2014.
- [31] Laurence Aitchison, Jannes Jegminat, Jorge Aurelio Menendez, Jean-Pascal Pfister, Alexandre Pouget, and Peter E Latham. Synaptic plasticity as bayesian inference. *Nature Neuroscience*, 24(4):565–571, 2021.
- [32] William B Levy and Robert A Baxter. Energy-efficient neuronal computation via quantal synaptic failures. *Journal of Neuroscience*, 22(11):4746–4755, 2002.
- [33] Daqing Guo and Chenguang Li. Stochastic resonance in hodgkin–huxley neuron induced by unreliable synaptic transmission. *Journal of theoretical biology*, 308:105–114, 2012.
- [34] Graeme W Davis and Martin Müller. Homeostatic control of presynaptic neurotransmitter release. *Annual review of physiology*, 77:251–270, 2015.
- [35] Corinna Wentzel, Igor Delvendahl, Sebastian Sydlik, Oleg Georgiev, and Martin Müller. Dysbindin links presynaptic proteasome function to homeostatic recruitment of low release probability vesicles. *Nature communications*, 9(1):1–16, 2018.
- [36] Rui Ponte Costa, Robert C Froemke, P Jesper Sjöström, and Mark CW van Rossum. Correction: Unified pre-and postsynaptic long-term plasticity enables reliable and flexible learning. *Elife*, 4:e11988, 2015.
- [37] Rui Ponte Costa, Beatriz EP Mizusaki, P Jesper Sjöström, and Mark CW van Rossum. Functional consequences of pre-and postsynaptic expression of synaptic plasticity. *Philosophical Transactions of the Royal Society B: Biological Sciences*, 372(1715):20160153, 2017.
- [38] Rui Ponte Costa, Zahid Padamsey, James A D’Amour, Nigel J Emptage, Robert C Froemke, and Tim P Vogels. Synaptic transmission optimization predicts expression loci of long-term plasticity. *Neuron*, 96(1):177–189, 2017.
- [39] Luke Campagnola, Stephanie C Seeman, Thomas Chartrand, Lisa Kim, Alex Hoggarth, Clare Gamlin, Shinya Ito, Jessica Trinh, Pasha Davoudian, Cristina Radaelli, et al. Connectivity and synaptic physiology in the mouse and human neocortex. *bioRxiv*, 2021.

A Appendix

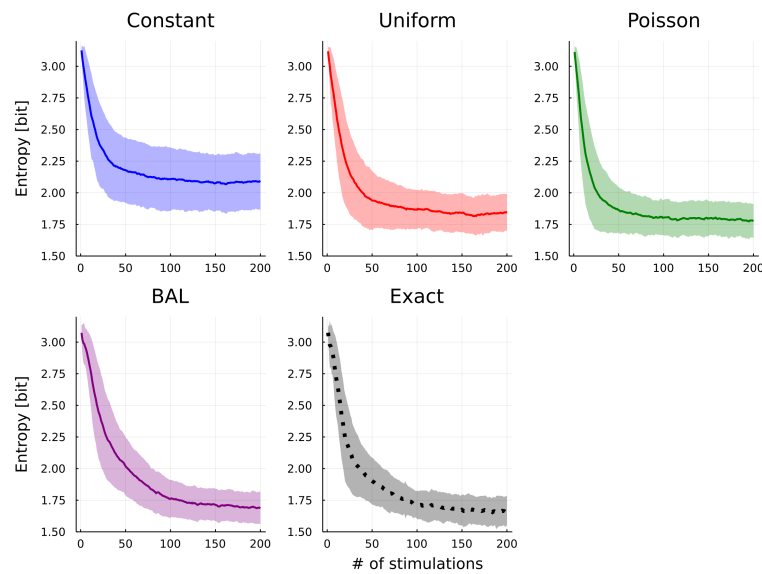


Figure 5: Same results as in Figure 3 (b). Shaded areas represent the standard deviations of results.